General synthesis of ferrocenylphosphine-bridged digold carboxylato complexes

Crystal and molecular structure of $Au_2(\eta^1\text{-}CF_3CO_2)_2(\mu\text{-dppf}) \cdot C_6H_{14}$ $(dppf = Fe(C_5H_4PPh_2)_2)$

Pauline M.N. Low [a], Ze-Ying Zhang [b], Thomas C.W. Mak [b], T.S. Andy Hor [a,*]

[a] Department of Chemistry, Faculty of Science, National University of Singapore, Kent Ridge, Singapore 119260, Singapore
[b] Department of Chemistry, The Chinese University of Hong Kong, Shatin, N.T., Hong Kong

Abstract

Metathesis of $Au_2Cl_2(\mu\text{-dppf})$ with $Ag(RCO_2)$ (R = CH_3, CF_3, C_2H_5 and C_6H_5) gives $Au_2(\eta^1\text{-}RCO_2)_2(\mu\text{-dppf})$ in 75–97% yields. Spectroscopic data are consistent with a common structure containing a ferrocenyl diphosphine bridging two moieties of Au(I) bearing carboxylates in a unidentate coordination mode. Similar reaction of $Au_2Cl_2(\mu\text{-dppm})$ with $Ag(CF_3CO_2)$ gives $Au_2(\eta^1\text{-}CF_3CO_2)_2(\mu\text{-dppm})$ in 52% yield. X-ray single-crystal crystallographic diffraction analysis of $Au_2(\eta^1\text{-}CF_3CO_2)_2(\mu\text{-dppf}) \cdot C_6H_{14}$ shows that in the centrosymmetric dinuclear molecule, the Au(I) geometry is approximately linear ($\angle$O–Au–P 177.1(1)°) and the trifluoroacetate ligand is unidentate (C(18)–O(1) 1.267(4)Å and C(18)–O(2/2a) 1.212(4)Å). An intermolecular Au...Au interaction of 3.254(1)Å links the molecules into an infinite zigzag chain running parallel to the c axis. Crystal data: $Au_2(\eta^1\text{-}CF_3CO_2)_2(\mu\text{-dppf}) \cdot C_6H_{14}$, space group $C2/c$ (No. 15), $a = 15.325(3)$, $b = 19.058(4)$, $c = 15.373(3)$Å, $\beta = 95.98(3)°$, final $R = 5.66\%$ for 3784 observed reflections. © 1997 Elsevier Science S.A.

Keywords: Metathesis; Phosphine bridges; Monophosphines

1. Introduction

Recent reports on diphosphine-bridged gold complexes have demonstrated some unusual inter- and intra-molecular bonding properties. For example, although $AuCl(PPh_3)$ [1] and $Au_2Cl_2(\mu\text{-dppe})$ [2,3] are mono- and dinuclear respectively, the structure of $[AuCl(\mu\text{-dppf})]_n$ (dppf = 1,1′-bis(diphenylphosphino)ferrocene) is dimeric [2] or polymeric [4] with strong interactions between discrete units of [AuCl(dppf)]. The propensity for polymerization through coordination expansion of linear-Au(I) to trigonal planar-Au(I) and formation of phosphine bridges is a complex molecular phenomenon. This, together with the possibilities for Au...Au intra- and inter-molecular interactions [5] and the interchange of bridging and terminal ligands in the basic core AuX(P–P) (X = halides and pseudohalides, P–P = diphosphine), give rise to some structural multiplicities to Au(I) diphosphine complexes. These bonding and geometric variations also make structural prediction difficult based solely on solution data. Many of the gold complexes exhibit exciting photophysical [6] and therapeutic [3–7] properties and have potential to be new materials [8]. In the course of our work on carboxylato complexes [9], we noticed that similar gold carboxylates, although showing some significant antitumor activities [10], are surprisingly ill-developed. To our knowledge, binary gold carboxylates are unknown whereas their phosphine complexes are confined to a few reports of the monophosphines. There is no crystallographic report on any digold carboxylate complexes.

* Corresponding author. Tel.: (+65) 7722917; fax: (+65) 7791691; e-mail: chmandyh@nus.sg.

In this paper, using dppf as an example, we wish to report a simple and general synthetic method and the first X-ray structural identification of a diphosphine-bridged digold carboxylate. The significance of dppf complexes of gold in biomedical chemistry has been described [11]. Mirabelli et al. [12] in a comprehensive study illustrated the possible involvement of 'metal chelation' in the antineoplastic mechanism and the importance of the metal proximity and role of the terminal ligands in the antitumor activities of the digold complexes. The authors reported the preparation of $Au_2(\eta^1\text{-}CH_3CO_2)_2(\mu\text{-dppe})$ as the only carboxylato complex. No detailed spectroscopic or crystallographic evidence has emerged in these species.

2. Results and discussion

The preparation of $Au_2(\eta^1\text{-}PhCO_2)_2(\mu\text{-dppf})$ from the metathesis of $Au_2(\eta^1\text{-}NO_3)_2(\mu\text{-dppf})$ with $Na^+PhCO_2^-$ was reported [4]. We have modified this procedure by using $Ag(PhCO_2)$ which allows a one-step synthesis directly from $Au_2Cl_2(\mu\text{-dppf})$. The latter can be obtained easily from $AuCl(SMe_2)$ and dppf. Using this modified procedure, $Au_2(\eta^1\text{-}RCO_2)_2(\mu\text{-dppf})$ (R = CH_3, CF_3, C_2H_5 and C_6H_5) and $Au_2(\eta^1\text{-}CF_3CO_2)(\mu\text{-dppm})$ can be prepared in yields between 52–97% (Eq. (1)).
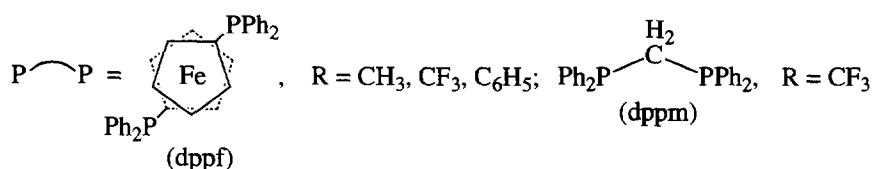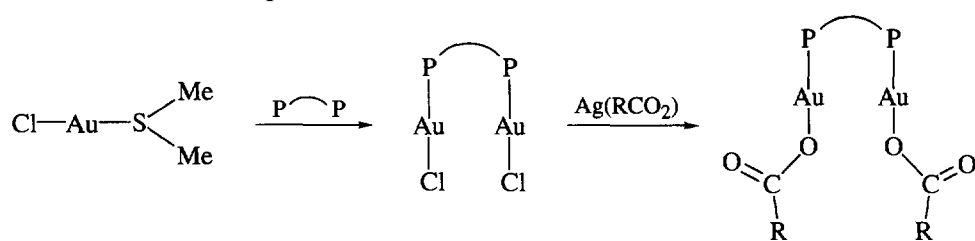
(1)

The use of other carboxylates when P–P = dppm gives complexes which are presently unidentified. The choice of $Ag(RCO_2)$ as a carboxylate source is common [13]. Methane elimination from $AuMe(PPh_3)$ with carboxylic acid is another possibility [14]. Gold(I) complexes with oxygen donors are rare in the literature. The title complexes are stable in solution. The nmr (^1H and ^{31}P) spectra are generally uninformative except showing the phosphine coordination and equivalence of the phosphine groups. The infrared data, based on $\Delta(\nu_{sym} - \nu_{asym})$, are indicative of the carboxylate groups in a monodentate coordination mode. These data are indicative of a diphosphine-bridged structure with Au(I) being linearly coordinated and carboxylate coordination through one of its oxygen atoms.

To verify the solid-state structure of the title carboxylates, we have carried out an X-ray single-crystal diffraction analysis of $Au_2(\eta^1\text{-}CF_3CO_2)_2(\mu\text{-dppf})$ which contains a hexane solvate. The crystallographic data and refinement details of $Au_2(\eta^1\text{-}CF_3CO_2)_2(\mu\text{-dppf})$ are summarized in Table 1; selected geometric data are listed in Table 2. The analogous $Au(CF_3CO_2)(PPh_3)$ has been obtained similarly from $AuCl(PPh_3)$ and $AgCF_3CO_2$ [13]. To date, a number of the known mononuclear Au(I) phosphine carboxylates, namely $Au(\eta^1\text{-}RCO_2)(PPh_3)$ (R = CH_3 [15], $CHCl_2$ [16], CF_3 [17], $HC(CH_3)_2$ [18], $HC(OH)CH_3$ and Ph [19]), have been crystallographically characterized. The digold structure (Fig. 1) shows a ferrocenyl diphosphine singly bridging two Au(I) centers with the Fe atom at a center of symmetry.

A monodentate trifluoroacetate group completes the coordination requirement of linear Au(I) ($\angle O\text{-}Au\text{-}P$ 177.1(1)°). The uneven C–O lengths of the carboxyl group (C(18)–O(1) 1.267(4) Å and C(18)–O(2/2a) 1.212(4) Å) with the stronger C–O bond associated with the pendant oxygen is a characteristic of monodentate carboxylate. With an anti-arrangement of the phosphine groups (twist angle $\tau = 180°$), there is no direct interaction between the gold atoms within the dinuclear unit. It is interesting to note that, in spite of the presence of pendant carboxyl oxygen, the dinuclear complex prefers an auriophilic [20] Au...Au to Au...O intermolecular aggregation. Close contacts of the type Au(1)...Au(1b) across a crystallographic two-fold axis link the molecules into an infinite zigzag chain running parallel to the c axis. A crystal packing diagram is shown in Fig. 2. The Au...Au contact of 3.254(1) Å is comparable to those found in other Au(I) pairing systems, e.g. $[Au_3(PPh_3)_3(\mu_3\text{-X})]BF_4$ (X = Te) (3.040(1) and 3.308(1) Å) [21] and NCN (3.098(1) and 3.316(1) Å) [22].

Table 1
Crystallographic data and refinement details for $Au_2(\eta^1\text{-}CF_3CO_2)_2(\mu\text{-dppf})\cdot C_6H_{14}$

Formula	$C_{44}H_{42}Au_2F_6FeO_4P_2$
Formula weight	1260.5
Color; habit	Yellow; prism
Crystal size (mm³)	0.15×0.20×0.60
Crystal system	Monoclinic
Space group	$C2/c$ (No. 15)
a (Å)	15.325(3)
b (Å)	19.058(4)
c (Å)	15.373(3)
β (deg)	95.98(3)
V (Å³)	4467(2)
Z	4
D_{calc} (Mg m⁻³)	1.874
Absorption coefficient (mm⁻¹)	7.010
$F(000)$	2424
Weighting scheme	$w^{-1} = \sigma^2(F)+0.0000F^2$
Observed data, n	3784 $(F > 6.0\sigma F)$
No. of variables, p	268
R (%)	5.66
R' (%)	6.73
S	1.85
Residual extrema in final difference map (e⁻ Å⁻³)	−1.58 to 1.75

$R = \Sigma\|F_o| - |F_c\|/\Sigma|F_o|.$
$R' = [\Sigma w^2(|F_o| - |F_c|)^2/\Sigma w^2|F_o|^2]^{1/2}.$

We have previously pointed out that in an open-bridging mode, the two phosphine groups of dppf are favored to deviate from the C_5 planes away from the iron center. This phenomenon is also observed in this complex with the phosphorus atoms deviating −0.1231 Å from the C_5 planes. This deviation is significantly higher than that found in $Au_2Cl_2(\mu\text{-dppf})\cdot CHCl_3$ (0.0068 Å and 0.029/0.041 Å in two crystallographically independent molecules). This deviation, however, does not affect the strength of the Au–P bonds. The observed Au–P lengths (2.219(2) Å) are shorter than those of the other Au(I) dimers (e.g. $Au_2Cl_2(\mu\text{-dppf})$ (mean 2.231(3) Å), [AuCl(μ-dppf)]$_n$ (mean Au–P 2.308(2) Å) and [$Au_2(\eta^2\text{-dppf})_2(\mu\text{-dppf})](NO_3)_2$ (Au–P_{bridge} 2.335(3) and Au–$P_{chelate}$ 2.389(3) Å)) and comparable with those in the mononuclear carboxylate analogs, e.g. $Au(\eta^1\text{-}CH_3CO_2)(PPh_3)$ (2.207(3) Å), $Au(\eta^1\text{-}CF_3CO_2)(PPh_3)$ (2.208(4) Å), $Au(\eta^1\text{-}(CH_3)_2CHCO_2)(PPh_3)$ (2.213(2) Å) and $Au(\eta^1\text{-}PhCO_2)(PPh_3)$ (2.213(3) Å). The Au–O bond (2.078(3) Å) is slightly shorter compared to that in $Au(\eta^1\text{-}CF_3CO_2)(PPh_3)$ (2.107(8) Å) both of which are longer than those found in other carboxylates, viz. $Au(\eta^1\text{-}CH_3CO_2)(PPh_3)$ (2.063(6) Å), $Au(\eta^1\text{-}CHCl_2CO_2)(PPh_3)$ (2.049(9) Å), $Au(\eta^1\text{-}(CH_3)_2CHCO_2)(PPh_3)$ (2.047(6) Å), $Au(\eta^1\text{-}(CH_3)(OH)CHCO_2)(PPh_3)$ (2.038(16) Å) $Au(\eta^1\text{-}PhCO_2)(PPh_3)$

Table 2
Selected bond lengths (Å), angles (deg) and least squares plane data of $Au_2(\eta^1\text{-}CF_3CO_2)_2(\mu\text{-dppf})\cdot C_6H_{14}$

Au(1)–P(1)	2.219(2)	Au(1)–O(1)	2.078(3)
C(18)–O(1)	1.267(4)	C(18)–O(2)	1.218(4)
C(18)–O(2')	1.206(3)	C(18)–C(19)	1.576(4)
C(19)–F(1–3)	1.331(4) (mean)	C(19)–F(1'–3')	1.336(4) (mean)
C(19)–F(1"–3")	1.333(4) (mean)	P(1)–C(5)	1.773(3)
P(1)–C(11)	1.815(3)	P(1)–C(17)	1.809(3)
Fe(1)–C(1–5)	2.051(3) (mean)		
Au(1)...Au(1a) (intramolecular)	8.645(2)		
Au(1)...Au(1b) (intermolecular)	3.254(1)		
P(1)–Au(1)–O(1)	177.1(1)	C(18)–O(1)–Au(1)	114.2(2)
O(1)–C(18)–O(2)	128.3(3)	O(1)–C(18)–O(2')	128.0(3)
O(1)–C(18)–C(19)	111.3(2)	O(2)–C(18)–C(19)	115.2(2)
O(2')–C(18)–C(19)	117.6(3)	C(18)–C(19)–F(1–3)	109.7(2) (mean)
C(18)–C(19)–F(1'–3')	110.4(2) (mean)	C(18)–C(19)–F(1"–3")	110.3(2) (mean)
Au(1)–P(1)–C(5)	113.1(1)	Au(1)–P(1)–C(11)	113.8(1)
Au(1)–P(1)–C(17)	112.4(1)		

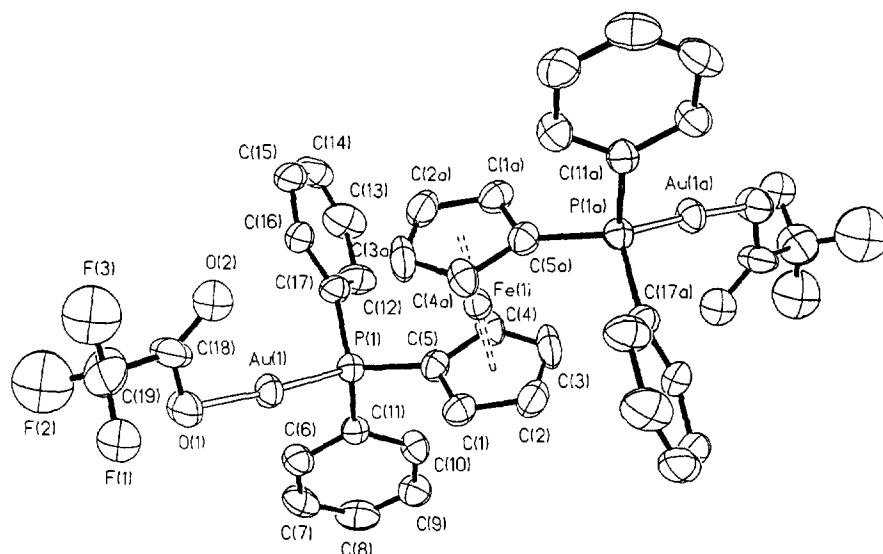Symmetry transformation: a = (1 − x, 1 − y, 1 − z); b = (1 − x, y, $\frac{1}{2}$ − z).

Fig. 1. Perspective view of the dinuclear $Au_2(\eta^1\text{-}CF_3CO_2)_2(\mu\text{-dppf})$ molecule in its crystalline hexane solvate. The thermal ellipsoids are drawn at the 35% probability level. For clarity the $O(2')$ atom is omitted, and the disordered CF_3 group is shown in one of its three possible orientations.

(2.033(6) Å). This suggests possible dissociation for $CF_3CO_2^-$ especially in the presence of strong σ-donors. In an open-bridging mode, dppf usually, but not necessarily, displays an ideal antiperiplanar (staggered) ($\tau = 180°$) conformation. For example, although dppf appears to be in an unrestricted open-bridging mode in $Fe_2(CO)_8(\mu\text{-dppf})$ ($\tau = 162.8°$) [23] and $Re_4(CO)_{18}(\mu\text{-dppf})$ ($\tau = 131.3°$) [24], the twist angles are far from ideal. Interestingly, in $Au_2Cl_2(\mu\text{-dppf}) \cdot CHCl_3$, there are two pseudopolymorphs in the solid-state with different conformations, namely antiperiplanar ($\tau = 180°$) and anticlinal ($\tau = 150°$). This 'twist deformation' is not evident in the title complex.

The title complexes serve as a ready source of $[Au_2(P-P)]^{2+}$ in view of the lability of the carboxylates. For example, $Au_2(\eta^1\text{-}CF_3CO_2)_2(\mu\text{-dppf})$ undergoes instantaneous addition reaction with dppf to give a mixture of products presently unidentified. Present work in our laboratory is targeted at the possible effects on the inter- and intra-molecular Au–Au interactions upon replacement of carboxylates by other nucleophiles.
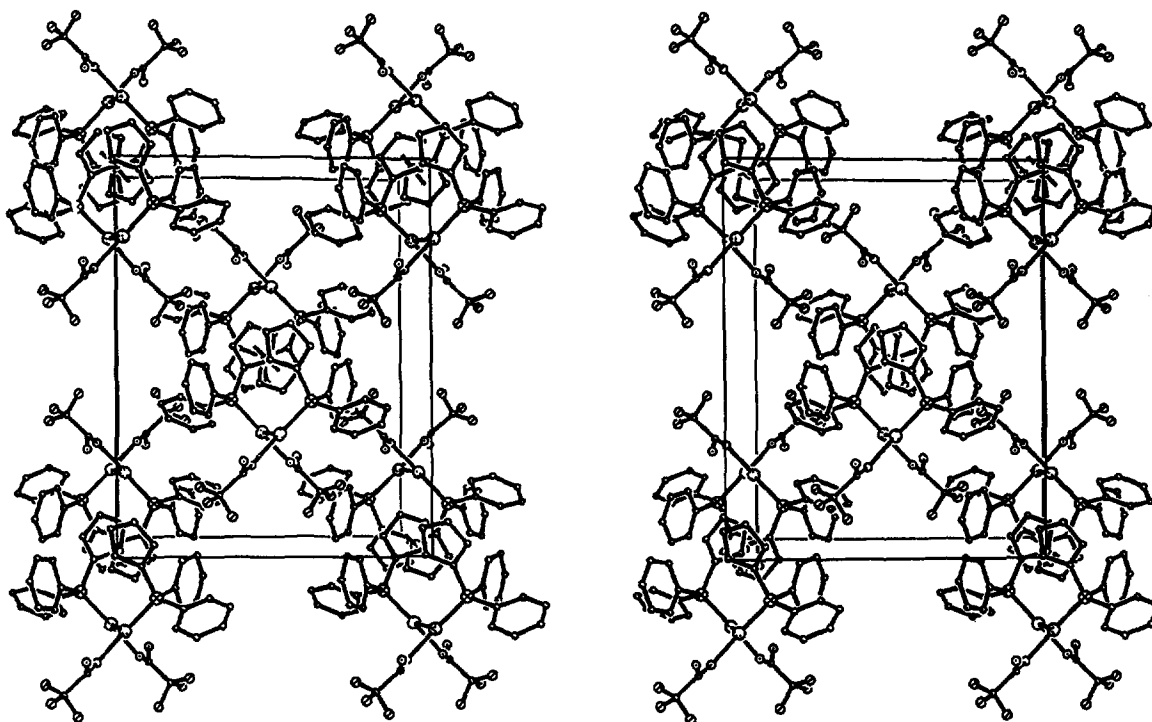

Fig. 2. Crystal packing diagram of $Au_2(\eta^1\text{-}CF_3CO_2)_2(\mu\text{-dppf})$ (origin at bottom left corner, a from left to right, b upward, and c toward reader).

3. Experimental section

3.1. General comments

All procedures were routinely performed at room temperature (27 °C) shielded from direct light and under pure dry argon, unless otherwise specified, with standard Schlenk techniques. The general procedures and instruments used followed those described earlier [25]. FT-IR spectra were obtained from KBr disc by using an FT-IR Perkin Elmer 1710 spectrometer. Molecular weight measurements were carried out by vapor pressure osmometry at Galbraith Laboratories, Inc., Knoxville, TN, USA. $Au_2Cl_2(\mu\text{-dppf})$ [3] and $Au_2Cl_2(\mu\text{-dppm})$ [26] were prepared by stoichio-metric addition of the diphosphine to $AuCl(SMe_2)$ [27]. $Fe(C_5H_4PPh_2)_2$ (dppf) was synthesized as reported [28].

3.2. Synthesis of $Au_2(\eta^1\text{-}CH_3CO_2)_2(\mu\text{-dppf})$

A mixture of $Au_2Cl_2(\mu\text{-dppf})$ (0.250 g, 0.245 mmol) and $Ag(CH_3CO_2)$ (0.091 g, 0.545 mmol) in CH_2Cl_2 (50 ml) was stirred at room temperature, shielded from direct light, for 24 h to give a light orange suspension. The reaction mixture was filtered through Celite to obtain a yellow-orange filtrate. The solvent was removed in vacuo and the orange residue extracted with CH_2Cl_2. Subsequent filtration through a column of Celite, followed by partial removal of solvent and addition of hexane to induce crystallization gave orange needles of $Au_2(\eta^1\text{-}CH_3CO_2)_2(\mu\text{-dppf})$ as a major product. Yield: 0.216 g, 82%. Anal. Calcd. for $C_{38}H_{34}Au_2FeO_4P_2$: C, 42.8; H, 3.2; Fe, 5.2; P, 5.8%. Found: C, 41.8; H, 3.3; Fe, 4.9; P, 5.8%. $\nu_{max}(CH_3CO_2^-)$: 1618 s, 1594 s, 1367 s, 1304 s cm^{-1} (KBr). δ_H: 2.05 (s, CH_3CO_2, 6H); 4.35 (sext, Cp_α, 4H); 4.86 (q, Cp_β, 4H); 7.37–7.56 (m, Ph, 20H) ppm. δ_P: 22.1 (s) ppm.

This general procedure was adopted to prepare the following complexes.

3.3. Synthesis of $Au_2(\eta^1\text{-}C_2H_5CO_2)_2(\mu\text{-dppf})$

$Au_2Cl_2(\mu\text{-dppf})$ (0.246 g, 0.241 mmol) and $Ag(C_2H_5CO_2)$ (0.100 g, 0.553 mmol) in CH_2Cl_2 (60 ml) gave golden orange flakes of $Au_2(\eta^1\text{-}C_2H_5CO_2)_2(\mu\text{-dppf})$ quantitatively. Yield: 0.253 g, 97%. Anal. Calcd. for $C_{39}H_{36}Au_2FeO_4P_2$: C, 43.4; H, 3.3; Fe, 5.1; P, 5.7%. Found: C, 42.5; H, 3.7; Fe, 4.8; P, 5.5%. $\nu_{max}(C_2H_5CO_2^-)$: 1618 vs(br), 1558 vs, 1374 s cm^{-1} (KBr). δ_H: 1.14 (t, H_a, 6H, $^3J_{H-H} = 7.5$ Hz); 2.33 (q, H_b, 4H, $^3J_{H-H} = 7.5$ Hz); 4.37 (sext, Cp_α, 4H); 4.84 (q, Cp_β, 4H); 7.37–7.57 (m, Ph, 20H) ppm. δ_P: 22.0 (s) ppm.

3.4. Synthesis of $Au_2(\eta^1\text{-}C_6H_5CO_2)_2(\mu\text{-dppf})$

$Au_2Cl_2(\mu\text{-dppf})$ (0.251 g, 0.246 mmol) and $Ag(C_6H_5CO_2)$ (0.120 g, 0.500 mmol) in CH_2Cl_2 (60 ml) gave golden orange flakes of $Au_2(\eta^1\text{-}C_6H_5CO_2)_2(\mu\text{-dppf})$ (0.219 g, 75%). Anal. Calcd. for $C_{48}H_{38}Au_2FeO_4P_2$: C, 48.4; H, 3.2; Fe, 4.7; P, 5.2%. Found: C, 48.0; H, 3.4; Fe, 4.2; P, 5.5%. $\nu_{max}(C_6H_5CO_2^-)$: 1610 s(br), 1572 m, 1329 vs(br) cm^{-1} (KBr). δ_H: 4.46 (m, Cp_α, 4H); 4.89 (q, Cp_β, 4H); 7.36–7.49 (m, Ph, 18H); 7.53–7.61 (m, Ph, 8H); 8.08–8.12 (m, Ph, 4H) ppm. δ_P: 22.3 (s) ppm.

3.5. Synthesis of $Au_2(\eta^1\text{-}CF_3CO_2)_2(\mu\text{-dppf})$

$Au_2Cl_2(\mu\text{-dppf})$ (0.292 g, 0.286 mmol) and $Ag(CF_3CO_2)$ (0.153 g, 0.693 mmol) in CH_2Cl_2 (50 ml) gave orange prisms of $Au_2(\eta^1\text{-}CF_3CO_2)_2(\mu\text{-dppf})$ (0.288 g, 88%). Anal. Calcd. for $C_{38}H_{28}Au_2F_6FeO_4P_2$: C, 38.9; H, 2.4; F, 9.7; Fe, 4.7; P, 5.3%. Found: C, 39.0; H, 2.7; F, 6.6; Fe, 4.4; P, 5.3%. M.W. found: 1132; calcd: 1174 (CHCl$_3$). $\nu_{max}(CF_3CO_2^-)$: 1695 s(br), 1404 m cm^{-1} (KBr). δ_H: 4.36 (sext, Cp_α, 4H); 4.86 (q, Cp_β, 4H); 7.37–7.56 (m, Ph, 20H) ppm. δ_P: 22.2 (s) ppm.

3.6. Synthesis of $Au_2(\eta^1\text{-}CF_3CO_2)_2(\mu\text{-dppm})$

$Au_2Cl_2(\mu\text{-dppm})$ (0.102 g, 0.120 mmol) and $Ag(CF_3CO_2)$ (0.060 g, 0.272 mmol) in CH_2Cl_2 (50 ml) gave off-white microcrystals of $Au_2(\eta^1\text{-}CF_3CO_2)_2(\mu\text{-dppf})$ (0.063 g, 52%). Anal. Calcd. for $C_{29}H_{22}Au_2F_6O_4P_2$: C, 34.7; H, 2.2; F, 11.4; P, 6.2%. Found: C, 33.8; H, 2.2; F, 10.2; P, 6.1%. $\nu_{max}(CF_3CO_2^-)$: 1696 s, 1684 s, 1406 m cm^{-1} (KBr). δ_H: 3.88 (t, CH_2, 2H, $^2J_{P-H} = 12.6$ Hz); 6.99–7.21 (m, Ph, 1H); 7.29–7.39 (m, Ph, 8H); 7.42–7.50 (m, Ph, 4H); 7.56–7.63 (m, Ph, 6H); 8.15–8.18 (m, Ph, 1H) ppm. δ_P: 23.4 (s) ppm.

3.7. X-ray crystallographic analysis

Single crystals of $Au_2(\eta^1\text{-}CF_3CO_2)_2(\mu\text{-dppf}) \cdot C_6H_{14}$ suitable for X-ray diffraction analysis were grown from CH_2Cl_2–hexane mixture at room temperature. Intensity data were measured on a Rigaku RAXIS-IIC imaging plate

Table 3
Atomic coordinates of $Au_2(\eta^1\text{-}CF_3CO_2)_2(\mu\text{-dppf})\cdot C_6H_{14}$

Atom	x	y	z	U_{eq}
Au(1)	52386(2)	69246(2)	35557(2)	540(1)
Fe(1)	5000	5000	5000	478(1)
P(1)	6238(1)	6086(1)	3794(1)	45(1)
C(1)	4923(2)	5034(2)	3670(2)	58(1)
C(2)	4796(2)	4333(2)	3937(2)	74(1)
C(3)	5563(2)	4138(2)	4498(2)	81(1)
C(4)	6157(2)	4695(2)	4557(2)	58(1)
C(5)	5782(2)	5262(2)	4037(2)	52(1)
C(6)	7050(2)	6448(2)	2319(2)	63(1)
C(7)	7538(2)	6327(2)	1637(2)	79(1)
C(8)	7795(2)	5668(2)	1456(2)	81(1)
C(9)	7578(2)	5110(2)	1962(2)	72(1)
C(10)	7099(2)	5225(2)	2674(2)	59(1)
C(11)	6844(2)	5910(2)	2863(2)	48(1)
C(12)	7900(2)	6035(2)	4736(2)	75(1)
C(13)	8521(2)	6208(2)	5442(2)	92(1)
C(14)	8286(2)	6621(2)	6073(2)	95(1)
C(15)	7453(2)	6897(2)	6032(2)	88(1)
C(16)	6848(2)	6740(2)	5332(2)	70(1)
C(17)	7065(2)	6299(2)	4680(2)	52(1)
C(18)	4028(2)	7924(2)	4098(2)	76(1)
O(1)	4321(2)	7729(2)	3395(2)	74(1)
O(2)	4014(2)	7597(2)	4777(2)	78(1)
O(2')	4378(2)	7876(2)	4835(2)	103(1)
C(19)	3282(2)	8490(2)	3917(2)	106(1)
F(1)	2680(2)	8300(2)	3268(2)	83(1)
F(2)	3702(2)	9057(2)	3663(2)	180(1)
F(3)	2890(2)	8640(2)	4618(2)	100(1)
F(1')	2922(2)	8570(2)	3106(2)	63(1)
F(2')	3603(2)	9104(2)	4226(2)	99(1)
F(3')	2646(2)	8300(2)	4419(2)	91(1)
F(1")	3318(2)	8825(2)	3157(2)	109(1)
F(2")	3290(2)	8969(2)	4544(2)	101(1)
F(3")	2532(2)	8130(2)	3880(2)	124(1)
C(20)	4030(2)	7271(2)	7374(2)	190(1)
C(21)	5000	7448(2)	7500	188(1)
C(22)	5190(2)	8105(2)	6989(2)	149(1)
C(23)	5000	8759(2)	7500	243(1)
C(24)	5089(2)	9414(2)	6942(2)	236(1)
C(25)	5000	10066(2)	7500	132(1)

[a] Equivalent isotropic U defined as one-third of the trace of the orthogonalized U_{ij} tensor.

diffractometer system [29] powered at 50 kV and 90 mA with Mo Kα radiation ($\lambda = 0.71073$ Å) monochromatized by highly oriented graphite crystal (25 frames, oscillation range (ϕ) 7.5°, and index ranges $-15 \leq h \leq 19$, $-15 \leq k \leq 24$, $-19 \leq l \leq 19$). The structure was solved with the Patterson superposition method with the aid of subsequent difference Fourier syntheses. The CF_3 group exhibits three-fold orientational disorder about the C(18)–C(19) bond. The hexane molecule is disordered about a crystallographic C_2 axis such that three of its six carbon atoms lie on it. One oxygen atom of the carboxylate group exhibits two-fold disorder and is represented by O(2) and O(2'). The distance restraints applied in least squares refinement are C–C 1.52 ± 0.01, C...C 2.50 ± 0.01, C–F 1.33 ± 0.01 F...F 2.17 ± 0.01 and C–O (in CO_2) 1.21 ± 0.01 Å. The final difference map contains residual extrema of $\pm 1.8\,e^-$ Å^{-3} in the neighborhood of the heavy gold atom. The iron atom is located at the center of symmetry, viz. Fe(1) at 1. All the non-hydrogen atoms were refined anisotropically. Hydrogen atoms of the organic ligands were generated geometrically (C–H = 0.95 Å), assigned isotropic thermal parameters, and allowed to ride on their parent carbon atoms. The phenyl groups on the phosphines were treated as rigid groups. The other non-hydrogen atoms were refined anisotropically, and the hydrogen atoms of the cyclopentadienyl groups were included in structure-factor calculations with assigned isotropic temperature factors. Atomic coordinate data for $Au_2(\eta^1\text{-}CF_3CO_2)_2(\mu\text{-dppf})$ are listed in Table 3. All computations were performed with the Siemens SHELXTL PLUS-PC program package [30]. Analytical expressions of neutral-atom scattering factors were employed, and anomalous-dispersion corrections were incorporated [31].

Acknowledgements

References

[1] N.C. Baenziger, K.M. Dittemore, J.R. Doyle, Inorg. Chem. 13 (1974) 805. W.E. Bennett, D.M. Soboroff, N.C. Baenziger, Acta Crystallogr. Sect. B: 32 (1976) 962.

[2] A. Houlton, R.M.G. Roberts, J. Silver, R.V. Parish, J. Organomet. Chem. 418 (1991) 269.

[3] D.T. Hill, G.R. Girard, F.L. McCabe, R.K. Johnson, P.D. Stupik, J.H. Zhang, W.M. Reiff, D.S. Eggleston, Inorg. Chem. 28 (1989) 3529.

[4] L.-T. Phang, T.S.A. Hor, Z.-Y. Zhou, T.C.W. Mak, J. Organomet. Chem. 469 (1994) 253.

[5] R.J. Puddephatt, J.J. Vittal, in R.B. King (Ed.), Encyclopedia of Inorganic Chemistry, vol. 3, Wiley, New York, 1994, p. 1320.

[6] D. Li, C.-M. Che, S.-M. Peng, S.-T. Liu, Z.-Y. Zhou, T.C.W. Mak, J. Chem. Soc. Dalton Trans. (1993) 189. S.-J. Shieh, D. Li, S.-M. Peng, C.-M. Che, J. Chem. Soc. Daltons Trans. (1993) 195.

[7] S.J. Berners-Price, G.R. Girard, D.T. Hill, B.M. Sutton, P.S. Jarrett, L.F. Faucette, R.K. Johnson, C.K. Mirabelli, P.F. Sadler, J. Med. Chem. 33 (1990) 1386. S.J. Berners-Price, P.J. Sadler, Struct. Bonding (Berlin) 70 (1988) 27.

[8] Md.N.I. Khan, J.P. Fackler Jr., S.P. Chum, A. Paquet, J. Polymer Sci. Part A: Polymer Chem. 31 (1993) 2353.

[9] T.S.A. Hor, S.P. Neo, C.S. Tan, T.C.W. Mak, K.W.P. Leung, R.-J. Wang, Inorg. Chem. 31 (1992) 4510. S.P. Neo, Z.-Y. Zhou, T.C.W. Mak, T.S.A. Hor, J. Chem. Soc. Dalton Trans. (1994) 3451. S.P. Neo, Z.-Y. Zhou, T.C.W. Mak, T.S.A. Hor, Inorg. Chem. 34 (1995) 520. A.L.C. Tan, P.M.N. Low, Z.-Y. Zhou, W. Zheng, B.M. Wu, T.C.W. Mak, T.S.A. Hor, J. Chem. Soc. Dalton Trans. (1996) 2207.

[10] D.T. Hill, R.K. Johnson, C.K. Mirabelli, Eur. Pat. Appl., EP 151046. D.T. Hill, R.K. Johnson, C.K. Mirabelli, US Patent 4766226.

[11] K.-S. Gan, T.S.A. Hor, in: A. Togni, T. Hayashi (Eds.), Ferrocenes—Homogeneous Catalysis, Organic Synthesis and Materials Science, VCH, Weinheim, 1995, Chapter 1, p. 3.

[12] C.K. Mirabelli, D.T. Hill, L.F. Faucette, F.L. McCabe, G.R. Girard, D.B. Bryan, B.M. Sutton, J.O.L. Barus, S.T. Crooke, R.K. Johnson, J. Med. Chem. 30 (1987) 2181.

[13] D.I. Nichols, A.S. Charleston, J. Chem. Soc. A: (1969) 2581.

[14] C.M. Mitchell, F.G.A. Stone, J. Chem. Soc. Dalton Trans. (1972) 102.

[15] P.G. Jones, Acta Crystallogr. Sect. C: 40 (1984) 1320.

[16] J. Skoweranda, W. Wieczorek, M. Bukowska-Stryzewska, A. Grodzicki, E. Szlyk, J. Crystallogr. Spectrosc. Res. 22 (1992) 527.

[17] Z.-Y. Zhang, E. Szlyk, G.J. Palenik, S.O. Colgate, Acta Crystallogr. Sect. C: 44 (1988) 2197.

[18] J.P. Fackler Jr., Md.N.I. Khan, C. King, R.J. Staples, R.E.P. Winpenny, Organometallics 10 (1991) 2178.

[19] P.G. Jones, Acta Crystallogr. Sect. C: 41 (1985) 905.

[20] H. Schmidbaur, Chem. Soc. Rev. 24 (1995) 391. H. Schmidbaur, Gold Bull. 23 (1990) 11. K. Angermaier, E. Zeller, H. Schmidbaur, J. Organomet. Chem. 472 (1994) 371.

[21] K. Angermaier, H. Schmidbaur, Z. Naturforsch. Teil B: 51 (1996) 879.

[22] W. Schneider, K. Angermaier, H. Schmidbaur, Z. Naturforsch. Teil B: 51 (1996) 801.

[23] T.-J. Kim, S.-C. Kwon, Y.-H. Kim, N.H. Heo, M.T. Teeter, Y. Yamano, J. Organomet. Chem. 426 (1991) 71.

[24] T.S.A. Hor, H.S.O. Chan, K.-L. Tan, L.-T. Phang, Y.K. Yan, L.-K. Liu, Y.-S. Wen, Polyhedron 10 (1991) 2437.

[25] P.M.N. Low, A.L.C. Tan, T.S.A. Hor, Y.-S. Wen, L.-K. Liu, Organometallics 15 (1996) 2595.

[26] H. Schmidbaur, A. Wohlleben, F. Wagner, O. Orama, G. Huttner, Chem. Ber. 110 (1977) 1748; Chem. Ber. 110 (1977) 2751; Chem. Ber. 110 (1977) 2758.

[27] F. Bonati, G. Minghetti, Gazz. Chim. Ital. 103 (1973) 373.

[28] J.J. Bishop, A. Davison, M.L. Katcher, D.W. Lichtenberg, R.E. Merrill, J.C. Smart, J. Organomet. Chem. 27 (1971) 241.

[29] J. Tanner, K.L. Krause, Rigaku J. 11 (1994) 4; Rigaku J. 7 (1990) 28. K.L. Krause, G.N. Phillips Jr., J. Appl. Crystallogr. 25 (1992) 146. M. Sato, M. Yamamoto, K. Imada, Y. Yatsube, N. Tanaka, T. Higashi, J. Appl. Crystallogr. 25 (1992) 348.

[30] G. Sheldrick, SHELXTL-PC, Program Package for X-ray Crystal Structure Determination, Siemens Analytical Instruments, Inc.: Karlsruhe, Germany, 1990.

[31] International Tables for X-ray Crystallography, vol. 4, Kynoch Press, Birmingham, UK, 1974, pp. 55, 99, 149.